Rocznik Ochrona Środowiska

Volume 25 Year 2023 ISSN 2720-7501 pp. 25-36

https://doi.org/10.54740/ros.2023.004 open access

Received: March 2023 Accepted: March 2023 Published: April 2023

Optimisation of the Aerodynamic Characteristics of H-Darrieus Vertical-axis Wind Turbines

Anatoliy Pavlenko[1], Hanna Koshlak[2], Borys Basok[3], Volodymyr Novikov[4]*

[1]*Kielce University of Technology, Poland*
https://orcid.org/0000-0002-8103-2578
[2]*Kielce University of Technology, Poland*
https://orcid.org/0000-0001-8940-5925
[3]*Institute of Engineering Thermophysics of the National Academy of Sciences of Ukraine, Ukraine*
https://orcid.org/0000-0002-8935-4248
[4]*Institute of Engineering Thermophysics of the National Academy of Sciences of Ukraine, Ukraine*
https://orcid.org/0000-0003-1062-7336

[*]*corresponding author's e-mail: apavlenko@tu.kielce.pl*

Abstract: This article presents a study of the aerodynamic characteristics of a small H-Darrieus wind turbine to optimise its design. The article proposes correlations between the blades' geometric and aerodynamic characteristics, optimising the blades' profile and their dimensions for various values of wind speed, aerodynamic forces, and rotational moments. The data obtained can be helpful in the design and study of low-power wind turbines operating at low wind speeds with variable directions.

Keywords: wind turbine, aerodynamic characteristic, blade profile optimisation

1. Introduction

According to the World Wind Energy Association (WWEA), the worldwide installed capacity of wind turbines will exceed 1 million megawatts by mid-2023. A significant share in the generation of this power belongs to small wind turbines, which are used mainly in distributed energy to supply small disparate facilities. (Mahmuddin 2017, Ahmadi-Baloutaki et al. 2014, Pavlenko 2018, Batista et al. 2018, Cho et al. 2018, Sakran et al. 2022, Mohan et al. 2019, Madi et al. 2022, Jie et al. 2020). Usually, they work in stand-alone public lighting systems without being connected to the main network. (Salih et al. 2018, Zhang et al. 2022, Osei et al. 2022, Pavlenko & Koshlak 2021, Pavlenko 2019, Wen et al. 2021). The efficiency of small wind power plants (WPPs) is quite comparable with high-power WPPs. Although the performance of a wind turbine in the general case depends on the size of the turbine blades, it is worth paying attention to an indicator as rotating blades cover the area A_1. The power is a function of the square of this area ($N = f(A_1^2)$). Therefore, a large turbine can be replaced by several small ones with the same total area A_1. This gives many advantages, primarily in the material consumption M, which is a function $M = f(A_1^3)$. The same power generated by small wind turbines will be ten times cheaper than powerful turbines. Additionally, small wind turbines can operate at lower wind speeds, and the performance of some types of small wind turbines does not depend on the wind direction. Wind energy can be used to generate electricity in urban areas. This trend is mainly observed in Europe, where integrating wind turbines into the built environment is impossible. New small wind turbines are under development (Karthikeyan et al. 2015, Pagnini et al. 2015, Papi et al. 2021, Arumugam et al. 2021, Ishugah et al. 2014) for this application, which is mainly looking for quiet and efficient devices in the turbulent and asymmetric wind flow. Along with the installation of wind turbines around and on buildings, there is also interest in building wind turbines where the technology is integrated into the building structure and even building-augmented wind turbines where the turbine is part of the building structure or façade. A wind turbine complements the structure of the building in this case to maximise the use of wind energy.

2. The Concept of Using Wind Turbines for Urban Development

The use of wind resources in urban areas is not a new idea. Urban wind turbines installed on buildings are located within the surface roughness layer, which, as a rule, exceeds the height of surface elements by 1-3 times. The unevenness of this environment causes turbulence in airflow (wind), reducing the power output of many commonly used small wind turbines. However, studies of wind movement around obstacles such as buildings have shown that air (wind) can also be accelerated as it passes over them. Therefore, when designing a wind turbine for placement on a building, one should consider how it affects the change in wind speed, wind shear effects, profile, and airflow parameters.

When flowing around a building, two separate air pressure fields (ΔP) are formed, which cause an increase in the flow velocity and the formation of two currents. The first field ΔP appears on the nave side of the building and is related to the local dynamic pressure, which increases with the height of the building. As a result, the airflow collapses into a standing vortex system at the base of the building, causing high wind speeds in this local area. The second type of flow is due to the difference ΔP between the low-pressure regions (leeward and side face) and the relatively high-pressure regions at the base of the windward face. Flow directly between these two areas or around the corners of a building can cause very high local air velocities (Figure 1).

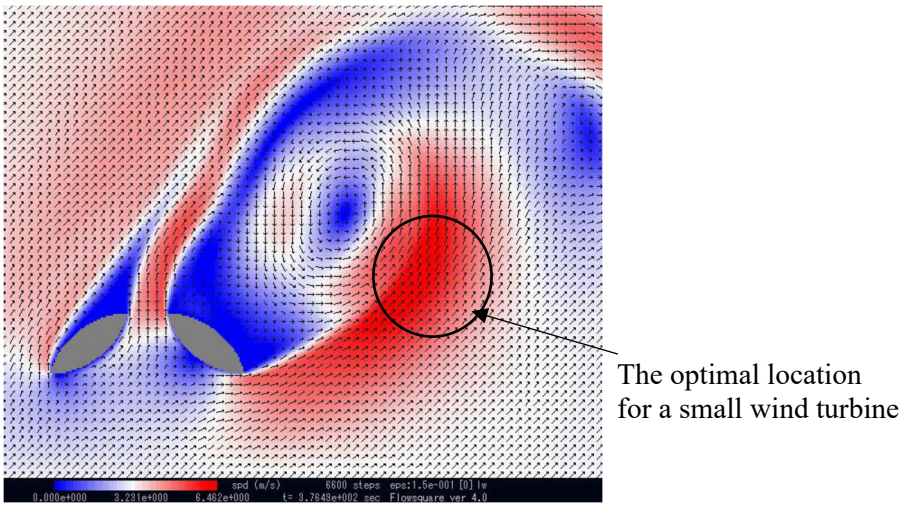

Fig. 1. Change the structure of the airflow when flowing around a building

The effects of wind shear on the buildings may depend on development at the district level. Placing a tall building in a low-rise area will cause wind shear effects. This will affect the local wind pattern. Figure 1 shows that due to the acceleration and shear of the airflow, local zones arise where wind turbines can be placed. Only the unresolved question of the optimal design of the wind power generator remains.

3. Optimisation of the Location of the Wind Turbine in Dense Urban Areas

In this part of the article, we propose an approach to integrating wind turbines into dense urban development, and we take individual buildings and structures for wind energy concentrators. On a specific example, based on the goals of CFD modelling, we studied the interaction of the wind flow with the complex of buildings and structures of the Institute of Engineering Thermophysics of the National Academy of Sciences of Ukraine to determine the most appropriate location of the wind power plant. The main objective of this study was to determine the rotor's aerodynamic characteristics and the wind turbine blade's optimal profile to power the experimental passive house.

Currently, there is a certain traditional algorithm for solving problems of assessing the energy potential of wind for the needs of wind energy:

- receiving and processing wind statistics of the target area;
- assessment of the energy characteristics of the wind flow using CFD modelling;
- choice of design and power of wind turbines.

In addition, we analysed the results of the numerical simulation of the airflow around the complex of adjacent buildings. The main tasks of the modelling were to determine the energy parameters of the wind flow in order to select a site for the most rational location of wind power plants. Also, the task of the study was to determine the external conditions near the building envelope for their subsequent use in the calculations of the heating and ventilation systems, as well as to determine the wind pressure on the building (especially high-rise) in terms of its strength characteristics and stability. The object of the study was the territory with a complex of administrative (non-residential) buildings of the Institute of Engineering Thermophysics of the National Academy of Sciences of Ukraine, located at the address: Kyiv, st. Academician Bulakhovsky, 2. Simulation of the airflow dynamics within urban areas is based on considering a sufficiently large area of the atmospheric boundary layer (ABL), the height of which, under the recommendations (Jorg et al. 2007), depends on the height of the tallest building. The air is assumed to be an incompressible medium, the airflow is turbulent, and the effect of Coriolis forces is negligible compared to the forces of air friction against the underlying surface to solve this problem. Just as in the construction of most models of the dynamics of air flows within the ABL

atmospheric boundary layer, the neutral stratification of the atmosphere over the area under consideration is assumed here, which makes it possible not to take into account the heat exchange between the air and the underlying Earth's surface.

Wind statistics. The initial data on the strength and direction of the wind in the study area correspond to the data of the meteorological station of the Kyiv airport, Kyiv, Zhuliany district. Wind speed and direction were carried out for two years with an average interval of 3 hours. Further processing of these data allowed us to build the corresponding wind rose (Fig. 2) and determine the average wind speed by 8 points at the height of the weather vane z_f = 10 m (Table 1). As seen from the above data, western, southwestern, and southern winds predominate in the study area on average per year. In the winter season (during the heating period), the winds are mainly western and northwestern. These data were correlated with the weather data from the departmental airfield of the aircraft manufacturing plant, located just a few kilometres from the study area.

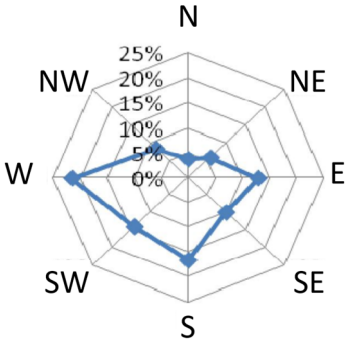

Fig. 2. Annual wind rose in the research area

Table 1. Direction and average wind speed in the target area

Rumb	N	NE	E	SE	S	SW	W	NW
Rose of Wind	4%	6%	13%	10%	17%	14%	21%	8%
Average wind speed, m/s	3.4	3.9	3.4	3.0	3.4	3.2	5.0	4.7

CFD modelling of wind currents in the target area. Air movement in the atmosphere obeys the fundamental equations of continuum mechanics. In this case, the Navier-Stokes system of equations of a viscous fluid motion, supplemented by two equations for the kinetic energy of turbulence and the dissipation of the kinetic energy of turbulence. The work (Tampieri et al. 2003) tested the standard k-ε turbulence model in CFD modelling of the wind potential of the Alaiz hill area in the province of Navarra (northern Spain) with a difference in the Earth's surface heights up to 1000 m above sea level. It is shown that the best agreement with the experimental data is given by the standard k-ε turbulence model using model constants.

Numerical modelling of wind flow in ABL. Numerical integration of the system of differential equations of viscous fluid dynamics is implemented in well-known CFD packages such as ANSYS Fluent, ANSYS CFX, Star CCM, PHOENICS, Open Form, and others. In recent decades, these packages have become widely used to model transport processes during air movement in the atmospheric boundary layer or, more precisely, in the surface part of the ABL. When constructing a CFD model of air movement in the surface layer of the atmosphere, four conditions must be met simultaneously (Jorg et al. 2007, Yang et al. 2009):

1) a sufficiently high resolution of the computational grid in the vertical direction near the Earth's surface;
2) horizontal uniformity of the wind flow in the solution area;
3) The distance z_p between the centres of the first layer of cells adjacent to the ground surface and the surface itself must be greater than the height of the physical (or geometric) roughness k_s, which is taken into account in CFD packages ($z_p > k_s$);
4) considering the height of the relationship between the physical roughness ks in CFD packages and the effective (aerodynamic) roughness of the Earth's surface z_0, on which the wind speed profile (1) depends.

Solution domain and grid model. The solution area of the CFD model to assess wind potential in the zone of compactly located building zone of ITTF NAS of Ukraine (Fig. 3) is built according to the recommendations (Jorg et al. 2007, Yossri et al. 2021), which determines the geometric dimensions of the solution area models depending on the height of the largest building. So, the entrance plane to the solution area should be 5-6 heights of the largest building from the first target buildings, the exit plane 7-9 heights, and the upper boundary can reach up to 4-5 heights.

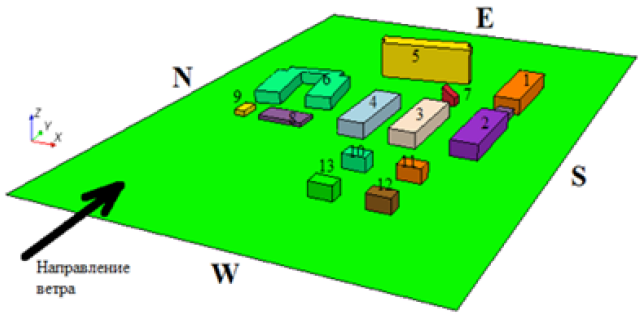

Fig. 3. Geometric model of the building complex

Buildings and structures are modelled by rectangles that preserve the buildings' main geometric dimensions and configuration.

1-4 – laboratory buildings (20×60×11 m); 5 – administrative building (71×17×29 m); 6 – pilot production – a complex configuration, in plan occupies a square of 60×60 m, the height of the building is 9 m, the distance between workshops is 20 m; 7 – an experimental house of passive type (10×8×13 m); 8 – garage (35×17×3 m); 9 – transformer electrical substation (8×15×4 m); 10-13 – warehouses (11×20×10 m). The dimensions of the solution area are x = 295 m, y = 420 m, z = 70 m.

When constructing the grid model, the power of modern computers and fairly versatile grid builders in CFD packages were taken into account, which allows the creation of grid models of almost any complexity with high resolution. At the same time, for reasons of computer time, to calculate one variant in CFD models of the wind flow in the surface layer for large solution areas, it is advisable to build non-uniform grids with a sufficiently high resolution near the Earth's surface. The height of the first layer of cells from the surface should not exceed 1-2 m.

For the purposes of this modelling, a tetrahedral mesh with a prismatic layer near the surfaces was built in the problem solution area, a fragment of which is shown in Fig. 4. The number of cells in the grid is about 6 million (5,968 thousand). The centres of the first layer of cells are located 1 m from the ground surface.

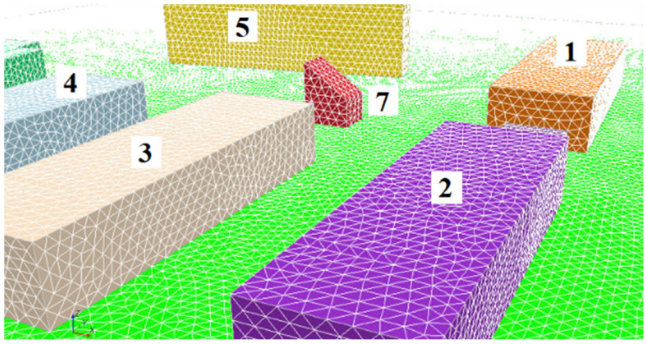

Fig. 4. A fragment of the computational grid of the model, in the centre there is a cut parallelepiped (7) – the contours of the experimental passive house "zero-energy" ITTF NAS of Ukraine. Designations of buildings correspond to the numbering in Fig. 3

Initial and boundary conditions of 3D CFD models. It is known that the vertical wind velocity profile above the underlying surface in an isotropic (homogeneous) boundary layer of the atmosphere can be described by logarithmic or power laws. Furthermore, as shown in (Richards & Hoxey 1993, Noronha & Krishna 2021, Singh & Ahmed 2013), no advantages of one law over another were found when compared with experimental data. However, in the same place (Richards & Hoxey 1993), it is shown that the logarithmic law is adequately applicable in the lower part of the ABL and the power law in the upper region. In the considered three-dimensional model, the logarithmic law of the velocity profile was used.

At the entrance to the solution region (the western boundary of the model, Fig. 4), the velocity profile and turbulence parameters of a fully developed turbulent horizontally homogeneous wind flow were set, formulated in (Wieringa et al. 2001b):

- change in the average wind speed in height;

$$U(z) = \frac{u_f}{\kappa} * \ln(\frac{z+z_0}{z_0}); \quad (1)$$

- the value of the kinetic energy of turbulence (KET);

$$k(z) = u_f^2/\sqrt{C_\mu}; \quad (2)$$

- the value of the dissipation of the kinetic energy of turbulence.

$$\varepsilon(z) = \frac{u_f^3}{\kappa}(z + z_0)^{-1}. \quad (3)$$

In formulas (1-3), κ = 0.41 is the Karman constant, uf is the friction velocity; z_0 is the parameter of the aerodynamic roughness of the surface of the Earth. The value of z_0 depends on the type of underlying surface (Blocken et al. 2007). The upper boundary of the solution area at the height of 70 m and the side boundaries (north and southern Fig. 4) were set as symmetry planes, which makes it possible to exclude wind velocity gradients at these boundaries and, accordingly, their influence on the target section of the model. At the exit of the solution region, the condition of the known normal atmospheric pressure P = 101325 Pa was established. The turbulence parameters were established for the return flow according to formulas (2), and (3). The lower boundary of the solution region was modelled as an impenetrable rough wall. For the Earth's surface, the standard wall function was used with a modification of the k_s-roughness of the sand. The roughness k_s and constant roughness C_S and E were consistent with the aerodynamic roughness z_0 according to the known relationship (ANSYS Fluent 2011):

$$k_s = \frac{Ez_0}{C_s}.$$

The standard wall function with zero height sand ks depth was also used on the surfaces of buildings and structures.

Calculation results. As a result of solving a numerical model of the interaction of the wind flow in the surface layer of the atmosphere with a complex of buildings and structures compactly located within urban areas, the fields of velocities, pressures, energy characteristics of the wind and other parameters of the wind flow were obtained. Below are the main simulation results for the direction of the west wind, the average speed of which at the height of the weather vane is 5 m/s (Table 1). The western wind direction is chosen as the most probable wind direction according to wind statistics (Fig. 2). As a result of solving a numerical model of the interaction of the wind flow in the surface layer of the atmosphere with a complex of buildings compactly located in the urban area, the fields of velocities, pressures and energy parameters of the wind were obtained.

One of the main goals of creating this model was to evaluate the turbulent and energy parameters of the wind flow to determine the most appropriate locations for the wind power plants needed to power the experimental passive house. There are two main types of wind turbines (wind turbines): traditional horizontal-axis wind turbines and vertical-axis wind turbines. It is known that the reliable operation of horizontal axial wind turbines depends quite strongly dependent on the turbulent characteristics of the wind flow. They work almost perfectly in the zone of undisturbed wind flow. The design features of vertical-axis wind turbines allow them to operate in any wind flow, including in local zones of acceleration and shear of the airflow, which are determined by the location of buildings and are observed in their immediate vicinity.

When assessing the characteristics of the wind flow in terms of its potential for wind power plants, first of all, the speed (1), (2) and, turbulent (3), (4) wind characteristics are evaluated:

– speed factor

$$K_v = \frac{U - U_{in}}{U_{in}}; \quad (4)$$

– wind flow-specific power

$$P_v = \frac{\rho U^3}{2}; \quad (5)$$

– normalised kinetic energy of turbulence

$$TKE = \frac{k}{U_{in}^2}; \quad (6)$$

– turbulence intensity

$$I_t = \frac{\sqrt{0.66k}}{U}, \quad (7)$$

where U is the local speed of the wind flow, m/s; U_{in} is the wind speed at the entrance to the solution area, m/s; k is the kinetic energy m^2/s^2; ρ – air density, kg/m^3.

Fig. 5 for flat sections of the model solution area at the height of 10, 20, and 30 meters shows the fields of values of the dimensionless wind speed coefficient K_v (4), which characterises the relative increase (decrease) in wind speed compared to the speed of the undisturbed flow at the entrance to the solution area.

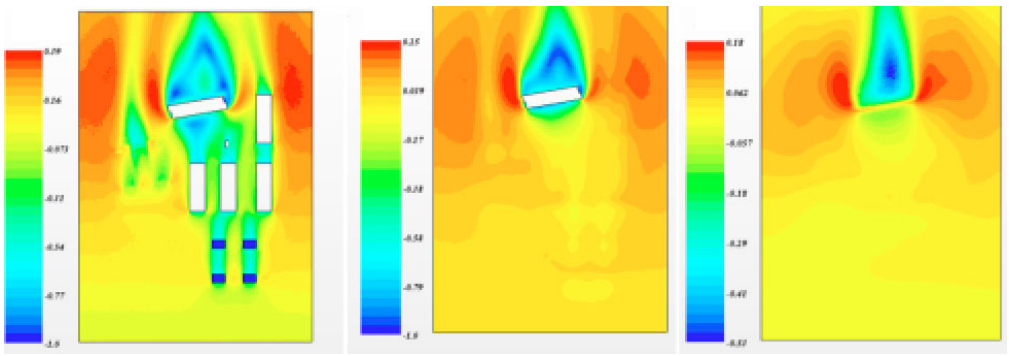

Z = 10 m; max K_v = 0.39 Z = 20 m, max K_v = 0,25; Z = 30 m, max K_v = 0,18

Fig. 5. Velocity fields at different heights

As can be seen from Fig. 5, already at the height of 30 m with a westerly wind, most of the target area is in the zone of a practically undisturbed wind flow, i.e. the influence of buildings and structures located on the surface of the Earth is minimal.

Fig. 6 shows a diagram of the most likely locations of wind turbines.

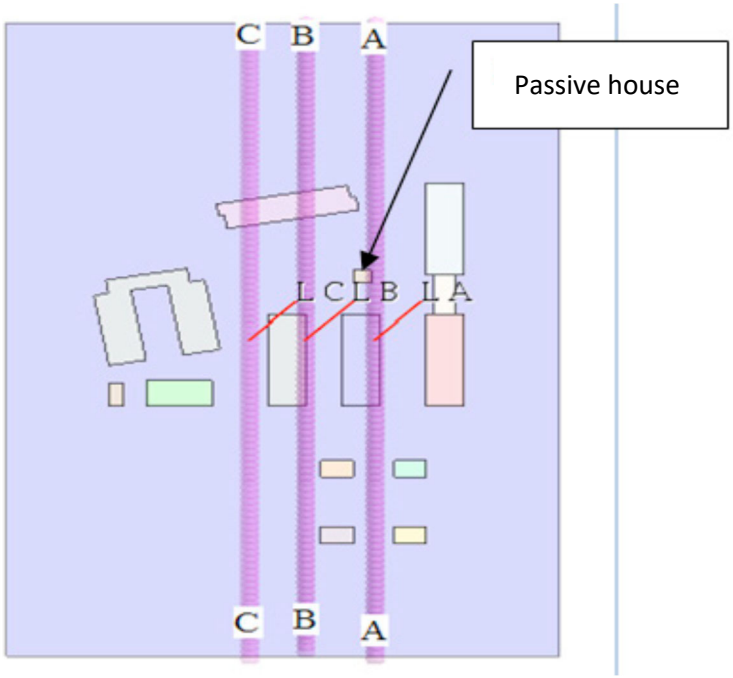

Fig. 6. Scheme of a rational arrangement of wind turbines and assessment of wind indicators

Considering the location of the passive house, Fig. 5, it is advisable to consider the energy and turbulent characteristics of the wind at the height of 30 m (this is the maximum possible mast height of a horizontal wind turbine, the installation of which does not require special permission) along the lines A-A, B-B and C-C. Fig. 7 shows a graph of changes in the specific power of the wind flow (5) along lines A-A, B-B and C-C.

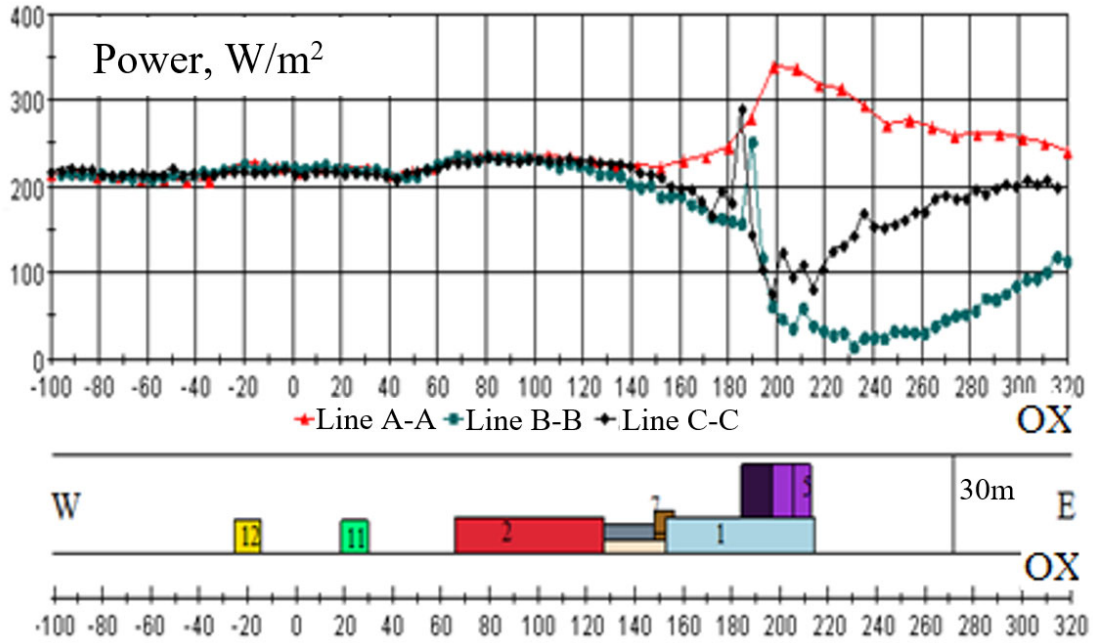

Fig. 7. Specific power of the wind flow at the height of 30 m along the rational areas of the wind turbine location

As can be seen from the graphs in Fig. 7 and the calculations performed, the specific power of the wind flow and its turbulent characteristics have almost the same values, starting from the inlet section of the solution area and up to building No. 2 for the three indicated in Fig. 5 possible installation lines. Moreover, the turbulent and energy characteristics of the wind in the area under consideration practically coincide with the corresponding indicators of the undisturbed wind flow, which is the most favourable factor for a horizontal-axial wind turbine.

As the wind approaches building No. 5 (the tallest building in the target area), the turbulent characteristics of the flow begin to increase sharply, and its energy performance decreases. This once again confirms the negative impact of turbulence on the operation of traditional horizontal axis wind turbines and the undesirability of their installation in areas of increased turbulence. Suppose we are talking about special designs of wind turbines intended for integration into urban development, for example, wind turbines of the H-Darrieus type with a vertical turbine rotor. In that case, the most successful location for such wind turbines will be in the area of the northern or southern ends of building No. 5 at the height of up to 10 m. This is evidenced by the data shown in Figs. 8, 9.

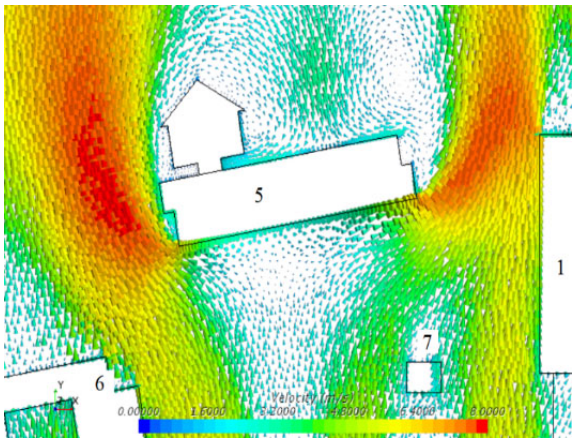

Fig. 8. Velocity field with a westerly wind in the area of a passive house at the height of 7 m

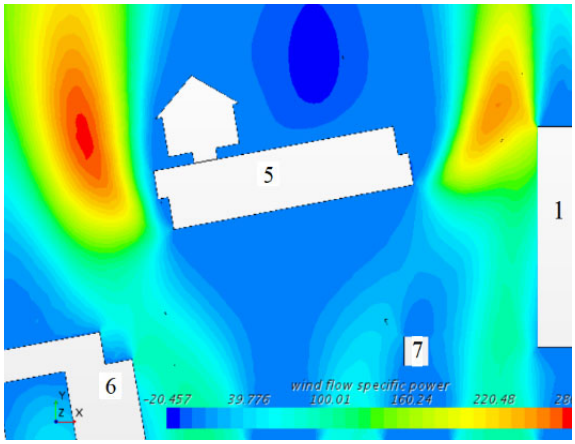

Fig. 9. The field of values of the specific power of the wind flow in the area of a passive house at the height of 7 m

In Fig. 9, you can see the shear and acceleration of the wind flow up to 8 m/s at the edges of the simulation tallest building in the target area. Note that the wind speed of the undisturbed flow at a weather vane height of 10 m is 5 m/s. The maximum values of the specific power of the wind turbine in the indicated zones in Fig. 8 confirm the probable installation sites of vertical-axial wind turbines.

4. Aerodynamic Characteristics of the H-Darrieus Wind Turbine

The article carried out studies of a small wind turbine located on the roof of the laboratory building of the Kielce University of Technology (Fig. 10).

The Darrieus rotor is a symmetrical structure with four aerodynamic wings mounted on radial beams. An aerodynamic force acts on each of the wings moving relative to the flow. It's magnitude depends on the angle between the flow velocity vectors and the wing's instantaneous velocity. This force reaches its maximum value when these vectors are orthogonal. Since the instantaneous velocity vector of the wing changes cyclically during the rotation of the rotor, the moment of force developed by the rotor is also variable. The rotor has a relatively small initial moment but a high speed (speed coefficient <3), due to this, a relatively large specific power. The lower wind power utilisation factor and efficiency are compensated for by the absence of energy losses when the wind direction changes. In the case of buffer storage of electricity, it is possible to reduce the requirements for the output voltage quality. At the same time, the required quality of electricity in the power supply channel can be ensured by standard devices for converting electrical energy (for example, uninterruptible power supplies such as UPS) with a battery of the appropriate capacity.

Although much attention has been paid to rotor designs by researchers (Ariefianto et al. 2023, Sadorsky 2021, Dąbek et al. 2019, Pavlenko 2014a), the task of optimising the shape of the blades remains relevant since the shape of the blades depends on specific aerodynamic conditions of the sites where the wind turbines are supposed to be placed.

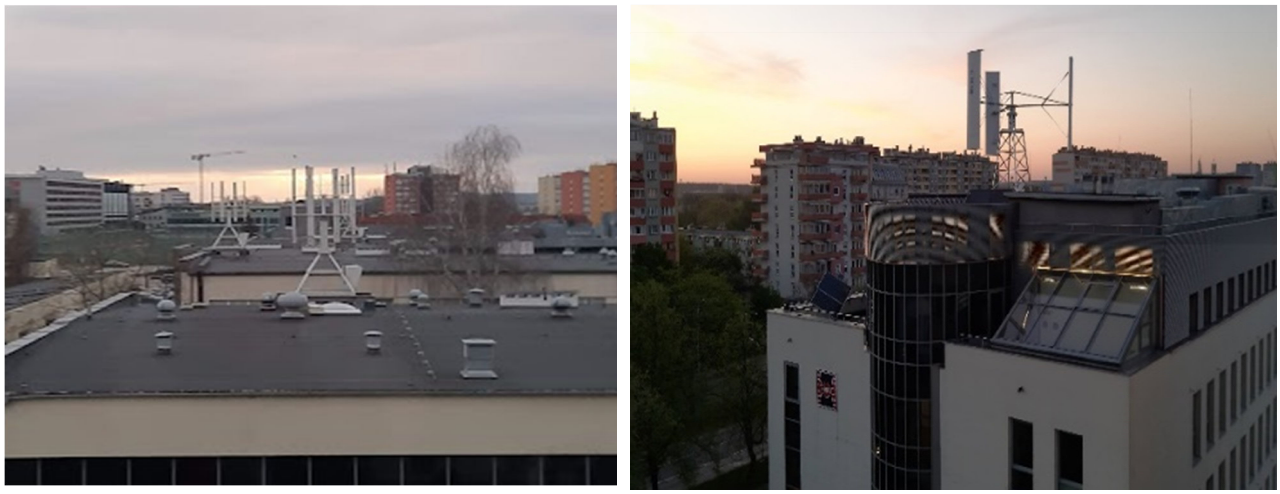

Fig. 10. Rotor H-Darrieus

In recent years, researchers have developed many methods and techniques (Bourhis et al. 2023, Piotrowski et al. 2014, Pavlenko et al. 2014a) to improve the efficiency of wind turbines based on accurate analysis and optimisation of the design parameters of wind turbine blades. The main limitation seen in VAWT is the high drag and turbulent force generated by the blade. In our studies, the NACA 0012-34 profile was chosen (Fig. 11), the shape of which was then optimised for the operating conditions of the wind turbine (Fig. 11). The NACA 0012-34 profile is selected and analysed in the required range of Reynolds numbers and wind speeds.

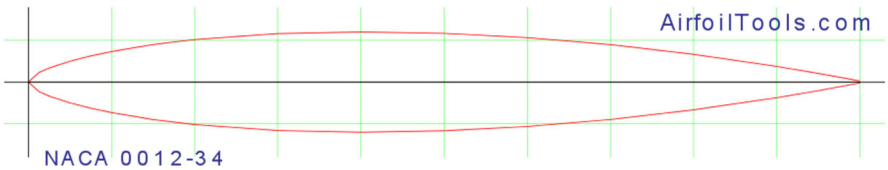

Fig. 11. Turbine blade profile H-Darrieus

The computational fluid dynamics (CFD) method was used for the theoretical analysis. A two-dimensional analysis was carried out to study a wind turbine blade's flow field. The results obtained for the drag and lift coefficients for several angles of attack were estimated from the available experimental data for the NACA 0012-34 aerofoil. The findings showed that CFD calculations could accurately calculate the flow around an aerofoil.

The lift and drag coefficients had to be determined to calculate the drag force (F_x) and the lift (F_y). The drag coefficient (C_x) and lift (C_y) forms can be written as follows:

$$C_x = \frac{2F_x}{A_1 \rho v^2}, \quad C_y = \frac{2F_y}{A_1 \rho v^2}. \tag{8}$$

To estimate the power of the wind turbine, we also determine the power factor (C_p)

$$C_p = \frac{(v_1^2 - v_2^2)(v_1 + v_2)}{2v_1^3}, \tag{9}$$

where v is the speed of the air flowing to the turbine, ρ, A_1 are the density of the air, the effective area of the object and the wind speed, respectively.

For the selected profile, the C_x/C_y ratios are shown in Figure 12.

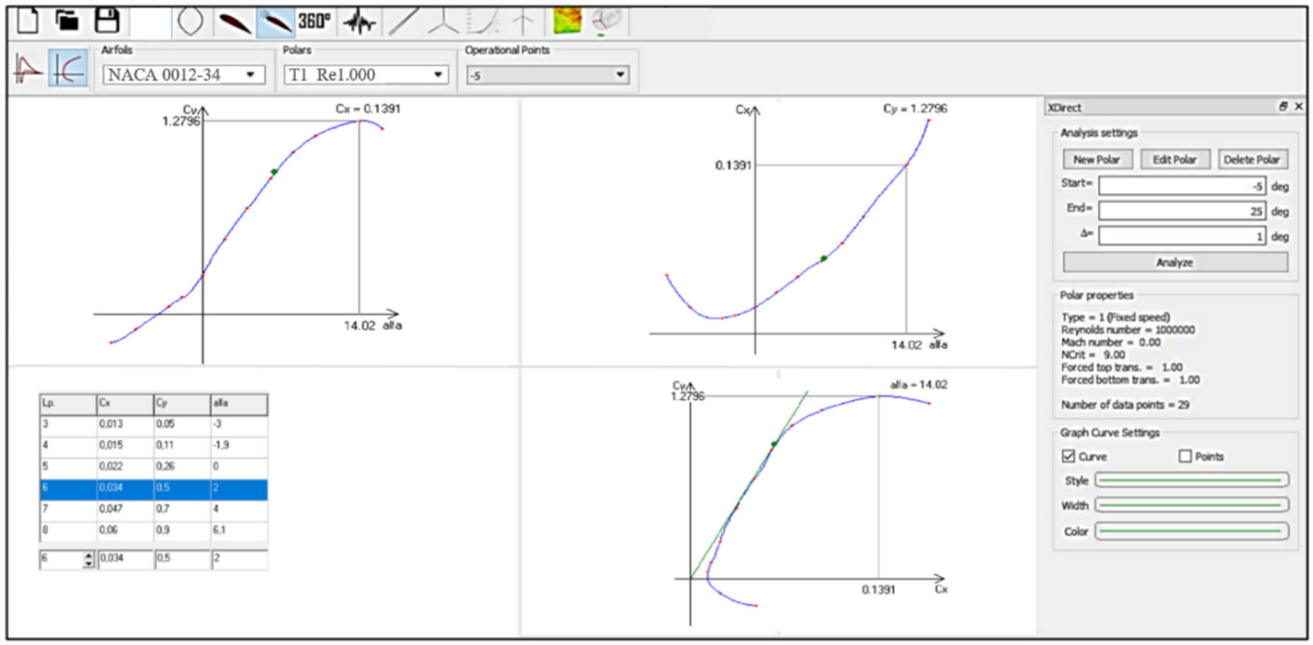

Fig. 12. Coefficients C_x, C_y, p and C_x/C_y ratio depending on the angle α (Fig. 13) for the NACA 0012-34 airfoil

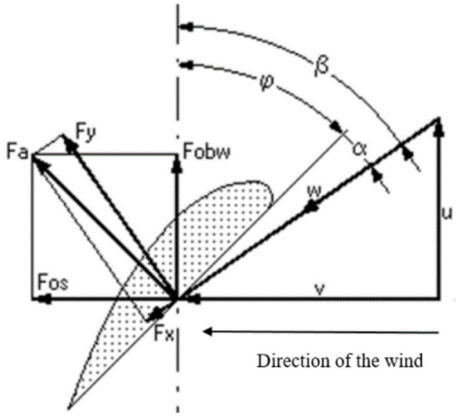

Fig. 13. Scheme of the interaction of the blade with the airflow

The next step was to optimise the airfoil's chord and twist angle to maximise the wind turbine's power output. For the NACA 0012-34 profile, which was taken as a base, the optimal angle α = 14.75, as seen in Fig. 12. This angle corresponds to the coefficients $C_x = 0.0623$, $C_y = 0.9375$, the power of the turbine with 4 blades is 1 kW. Fig. 12 shows the change in C_x, C_y, C_x/C_y depending on the angle of attack. The view from the operating point visualises the boundary layer and the generated pressure, as shown in Fig. 14. To complete the optimisation, the maximum value of C_x/C_y must be reached. The maximum value of C_x/C_y from Fig. 14 in the present analysis, the developed power of the same turbine with optimised blades, is 1.43 kW.

Figure 15 shows the power factor before and after the optimisation process.

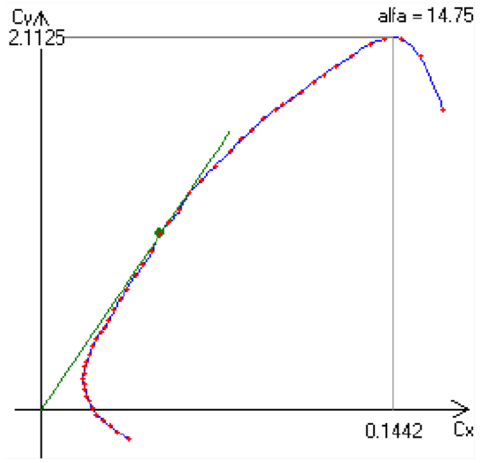

a)

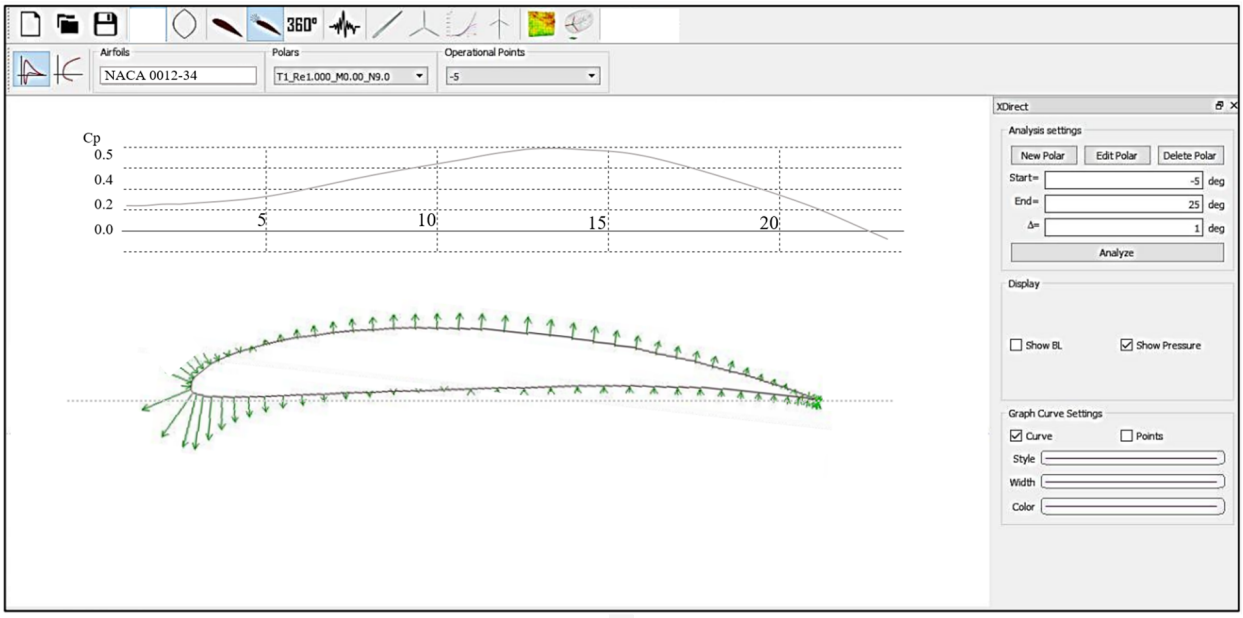

b)

Fig. 14. Optimised profile and power factor: a – C_x/C_y, b – optimised turbine blade profile

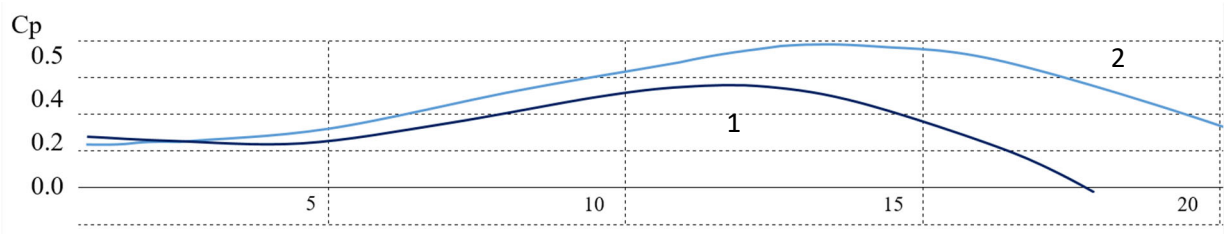

Fig. 15. Power factor before (1) and after (2) chord optimisation

5. Conclusions

The wind turbine design is always based on wind direction and speed data, which are measured for a specific area with a specific topography. Converting measured data to specific locations is not straightforward. Wind projects and related literature often lack specific information about the surrounding topography and roughness of adjacent areas of the building where the wind turbine is to be installed. However, as shown in this work, in certain local zones, the characteristics of the wind can differ significantly from the data from the climatic stations. It is advisable to use this feature to install small wind farms, having previously performed an airflow analysis using simulation software. Then, taking into account the small value of vertical vibration displacements in the resonances of the natural frequencies of the rotor and the supporting structure of the wind turbine, small installations can be placed not only close to residential buildings but also directly on the roof of

buildings and structures, greatly expanding the scope of this design. This paper demonstrates an approach that makes it possible to design a wind turbine for placement on the roof of a building while optimising the design of the blades of a standard H-Darrieus turbine. With the help of theoretical studies to optimise the design parameters, the main aerodynamic characteristics of the rotor and the optimal blade profile were determined. The power of a standard turbine can be increased by 40% due to optimisation.

References

Ahmadi-Baloutaki, M, Carriveau, R, Ting, DS-K. (2014). Straight-bladed vertical axis wind turbine rotor design guide based on aerodynamic performance and loading analysis. *Proceedings of the Institution of Mechanical Engineers, Part A: Journal of Power and Energy*, *228*(7), 742-759. https://doi.org/10.1177/0957650914538631

ANSYS FLUENT Theory Guide. Release 14.0, November 2011.

Ariefianto, Rizki, Mendung, Ariefianto, Rizki, Mendung, Hasanah, Rini, Nur, Hasanah, Rini, Nur, Wijono, W. (2023). Optimasi Turbin Arus Laut Tipe V-Shaped Blade dengan Mempertimbangkan Blade Aspect Ratio dan Solidity. *Jurnal Teknologi, 15*(1), 1-12. https://doi.org/10.24853/jurtek.15.1.1-12

Arumugam, P., Ramalingam, V., Bhaganagar, K. (2021). A pathway towards sustainable development of small capacity horizontal axis wind turbines – Identification of influencing design parameters & their role on performance analysis. *Sustain. Energy Technol. Assessments.*, *44*, Article 101019. https://doi.org/10.1016/j.seta.2021.101019

Batista, N., Melicio, R., Mendes, V. (2018). Darrieus-type vertical axis rotary-wings with a new design approach grounded in double-multiple streamtube performance prediction model. *AIMS Energy*, *6*(5), 673-694. https://doi.org/10.3934/energy.2018.5.673

Blocken, Bert, Stathopoulos, Ted, Carmeliet, J. (2007). CFD simulation of the atmospheric boundary layer: wall function problems. *Atmospheric Environment*, *41*(2), 238-252. © Elsevier 2007.

Bourhis, M., Pereira, M., Ravelet, F. (2023). Experimental investigation of the effect of blade solidity on micro-scale and low tip-speed ratio wind turbines. *Experimental Thermal and Fluid Science*, *140*, 110745. https://doi.org/10.1016/j.expthermflusci.2022.110745

Cho, S-Y, Choi, S-K, Kim, J-G, Cho, C-H. (2018). An experimental study of the optimal design parameters of a wind power tower used to improve the performance of vertical axis wind turbines. *Advances in Mechanical Engineering*, *10*(9). https://doi.org/10.1177/1687814018799543

Dąbek, L., Kapjor, A., Orman, Ł.J. (2019). Distilled water and ethyl alcohol boiling heat transfer on selected meshed surfaces. *Mechanics & Industry*, *20*, 701. https://doi.org/10.1051/meca/2019068

Ishugah, T.F., Li, Y., Wang, R.Z., Kiplagat, J.K. (2014). Advances in wind energy resource exploitation in urban environment : A review Renew. *Sustain. Energy Rev.*, *37*, 613-626. https://doi.org/10.1016/j.rser.2014.05.053

Jorg, Franke, Antti, Hellsten, Heinke, Schlunzen, Bertrand, Carissimo, (2007). *Best practice guideline for the cfd simulation of flows in the urban environment cost action 732 quality assurance and improvement of microscale meteorological models*. © COST Office. Available online: www.cost.esf.org.

Karthikeyan, N., Murugavel, K.K., Kumar, S.A., Rajakumar, S. (2015). Review of aerodynamic developments on small horizontal axis wind turbine blade. *Renew. Sustain. Energy Rev.*, *42*, 801-822, https://doi.org/10.1016/j.rser.2014.10.086

Mahmuddin, Faisal, (2017). Rotor Blade Performance Analysis with Blade Element Momentum Theory. *Energy Procedia*, *105*, 1123-1129. https://doi.org/10.1016/j.egypro.2017.03.477

Madi, Madi., Rahmawati, S., Mukhtasor., Satrio, D., Yasim, A. (2021). *Variation Number of Blades for Performance Enhancement for Vertical Axis Current Turbine in Low Water Velocity in Indonesia*. [In:] Proceedings of the 7th International Seminar on Ocean and Coastal Engineering, Environmental and Natural Disaster Management – ISOCEEN, ISBN 978-989-758-516-6, 47-53. https://doi.org/10.5220/0010047900470053

Mohan, Kumar, P., Sivalingam, K., Lim, T.-C., Ramakrishna, S., Wei, H. (2019). Review on the Evolution of Darrieus Vertical Axis Wind Turbine: Large Wind Turbines. *Clean Technol., 1*, 205-223. https://doi.org/10.3390/cleantechnol1010014

Noronha, N.P., Krishna, M. (2021). Aerodynamic performance comparison of airfoils suggested for small horizontal axis wind turbines. *Mater. Today Proc.*, *46*, 2450-2455. https://doi.org/10.1016/j.matpr.2021.01.359

Osei, Emmanuel, Yeboah, Opoku, Richard, Sunnu, Albert, K., Adaramola, Muyiwa, S., Kyeremeh, Ebenezer, Adu. (2022). Aerodynamic performance characteristics of EYO-Series low Reynolds number airfoils for small wind turbine applications. *Alexandria Engineering Journal*, *61*(12), 12301-12310. https://doi.org/10.1016/j.aej.2022.05.049

Pagnini, L.C., Burlando, M., Repetto, M.P. (2015). Experimental power curve of small-size wind turbines in turbulent urban environment. *Appl. Energy*, *154*, 112-121. https://doi.org/10.1016/j.apenergy.2015.04.117.

Papi, F., Nocentini, A., Ferrara, G., Bianchini, A. (2021). On the use of modern engineering codes for designing a small wind turbine: an annotated case study. *Energies*, *14*, 1-23. https://doi.org/10.3390/en14041013

Pavlenko, A.M. (2018). Dispersed phase breakup in boiling of emulsion. *Heat Transfer Research*, *49*(7), 633-641. https://doi.org/10.1615/HeatTransRes.2018020630.

Pavlenko, A.M. (2019). Energy conversion in heat and mass transfer processes in boiling emulsions. *Thermal Science and Engineering Progress*, *15*, 1-8. https://doi.org/10.1016/j.tsep.2019.100439

Pavlenko, A.M., Koshlak, H. (2021). Application of thermal and cavitation effects for heat and mass transfer process intensification in multicomponent liquid media. *Energies*, *14*(23), 7996. https://doi.org/10.3390/en14237996

Pavlenko, A.M., Koshlak, H., Usenko, B. (2014a). The processes of heat and mass exchange in the vortex devices. *Metallurgical and Mining Industry*, *6*(3), 55-59.

Pavlenko, A., Koshlak, H., Usenko, B. (2014b). Heat and mass transfer in fluidised layer. *Metallurgical and Mining Industry*, *6*(6), 96-100.

Piotrowski, J.Zb., Orman, Ł.J., Lucas, X., Zender-Świercz, E., Telejko, M., Koruba, D. (2014). *Tests of thermal resistance of simulated walls with the reflective insulation*. Proc. of Int. Conf. "Experimental Fluid Mechanics 2013", EPJ Web of Conferences, 67, 02095. https://doi.org/10.1051/epjconf/20146702095

Richards, P., Hoxey, R., (1993). Appropriate boundary conditions for computational wind engineering models using the k–ε turbulence model. *Journal of Wind Engineering and Industrial Aerodynamics*, *46-47*, 145-153.

Sadorsky, P. (2021). Wind energy for sustainable development : Driving factors and future outlook. *J. Clean. Prod.*, *289*, Article 125779. https://doi.org/10.1016/j.jclepro.2020.125779

Sakran, H.K., Abdul Aziz, M.S., Abdullah, M.Z. et al. Effects of Blade Number on the Centrifugal Pump Performance: A Review. Arab J Sci Eng 47, 7945–7961 (2022). https://doi.org/10.1007/s13369-021-06545-z

Salih, N., Akour, Mohammed, Al-Heymari, Talha, Ahmed, Kamel, Ali, Khalil. (2018). Experimental and theoretical investigation of micro wind turbine for low wind speed regions. *Renewable Energy*, *116*, Part A, 215-223. https://doi.org/10.1016/j.renene.2017.09.076

Singh, R.K., Ahmed, M.R. (2013). Blade design and performance testing of a small wind turbine rotor for low wind speed applications. *Renewable Energy*, *50*, 812-819. https://doi.org/10.1016/j.renene.2012.08.021

Su, Jie, Chen, Yaoran, Han, Zhaolong, Zhou, Dai, Bao, Yan, Zhao, Yongsheng, (2020). Investigation of V-shaped blade for the performance improvement of vertical axis wind turbines. *Applied Energy*, *260*, 114326, https://doi.org/10.1016/j.apenergy.2019.114326

Tampieri, F., Mammarella, I., Maurizi, A. (2003). Turbulence in Complex Terrain. *Boundary-Layer Meteorology*, *109*, 85-97. https://doi.org/10.1023/A:1025487702985

Wen, Q., He, X., Lu, Z., Streiter, R., Otto, T. (2021). A comprehensive review of miniatured wind energy harvesters. *Nano Mater. Sci.*, *3*, 170-185, https://doi.org/10.1016/j.nanoms.2021.04.001

Wieringa, J., Davenport, A.G., Grimond, B., Oke, Tim, R. (2001). *New revision of Davenport roughness classification*. 3rd European & African Conference on Wind Engineering. Eindhoven, Netherlands. Available online: http://www.kcl.ac.uk/ip/suegrimmond/ published papers/DavenportRoughness2.pdf

Yang, Yi, Gu, Ming, Jin, Xinyang. (2009). *New inflow boundary conditions for modeling the neutral equilibrium atmospheric boundary layer in sst k-ω model*. The Seventh Asia-Pacific Conference on Wind Engineering, November 8-12 2009, Taipei, Taiwan.

Yossri, W., Ayed, S. Ben, Abdelke, A. (2021). Airfoil type and blade size effects on the aerodynamic performance of small-scale wind turbines : Computational fluid dynamics investigation. *Energy*, *229*, 120739. https://doi.org/10.1016/j.energy.2021.120739

Zhang, Hongfu, Wen, Jiahao, Zhan, Jian, Xin, Dabo, (2022). Effects of blade number on the aerodynamic performance and wake characteristics of a small horizontal-axis wind turbine. *Energy Conversion and Management*, *273*, 116410. https://doi.org/10.1016/j.enconman.2022.116410